A Novel Near-Transparent ASK-Reconfigurable Inkjet-Printed Chipless RFID Tag

Arnaud Vena, *Member, IEEE*, Abdul Ali Babar, *Student Member, IEEE*, Lauri Sydänheimo, *Member, IEEE*, M. M. Tentzeris, *Fellow, IEEE*, and Leena Ukkonen, *Member, IEEE*

***Abstract*—The design of a novel chipless radio frequency identification (RFID) tag, which is inkjet-printed on a polyimide substrate, is presented. It is shown that a silver nanoparticles-based ink can be combined with a resistive organic ink to create a tag having a "near-transparent" configuration. By adding some transparent elements, we obtain various electromagnetic responses for tags visually similar. The tag is composed of three dual-rhombic loop resonators for a total size of 7×4 cm^2. It operates within the ultrawideband frequency range of 3–6 GHz. The resistive properties of the organic ink enable the implementation of a novel coding technique based on amplitude shift keying. Simulation and measurement results validate the concept and the novel coding technique.**

***Index Terms*—Anti-counterfeiting, backscattering, carbon nanotube (CNT) ink, chipless radio frequency identification (RFID), inkjet printing, resistive strips, silver nanoparticles ink, transparent.**

I. Introduction

RADIO frequency identification (RFID) technology appeared for the first time during World War II. It allowed remote recognition of friend and foe aircraft with the help of electromagnetic (EM) waves. The basic principle of the RFID technologies [1] relies upon the possibility to extract an identifier from a modulated radio frequency signal reflected (in passive systems) or transmitted (in active systems) by a transponder commonly known as an RFID tag. The detection reliability and the possibility to read a tag up to several tens of meters and non-line-of-sight (NLOS) are the main advantages of RFID compared to optical barcode technology. In addition, the passive tags do not require any internal power source to operate, other than the one radiated by the reader antenna. The chipless RFID technology [2]-[5], also called "RF barcodes," on the other hand drastically reduces the overall cost of the tag, compared to conventional chip-integrated RFID tags. A chipless RFID tag is usually composed of one or more conductive layers and does not require any lumped components. Thus, it can be entirely realized by a printing process. The extraction of an identifier (ID) relies on the analysis of its static backscattered EM response. Typically, these tags can be analyzed in time [2] and frequency [3]-[5] domains.

In this letter, we present the realization of a chipless tag with inkjet printing using both conductive and resistive inks. First, the chipless tag is inkjet-printed with the help of a conductive ink, consisting of silver nanoparticles, to achieve good radiating performance. Then, a transparent carbone nanotube (CNT)-doped organic (PEDOT) resistive ink is printed on top the tag to achieve a "near-transparent" tag configuration, beneficial for anti-counterfeiting applications. The resistive properties of the organic ink enable us to utilize a novel approach of using amplitude shift keying (ASK) technique to increase the coding efficiency.

Manuscript received February 18, 2013; revised April 22, 2013; accepted May 30, 2013. Date of publication June 21, 2013; date of current version July 10, 2013. This work was supported by the Finnish Funding Agency for Technology and Innovation, the Academy of Finland, and the Centennial Foundation of Finnish Technology Industries.

A. Vena, A. A. Babar, L. Sydänheimo, and L. Ukkonen are with the Tampere University of Technology, 33720 Tampere, Finland (e-mail: arnaud.vena@tut.fi; abdul.babar@tut.fi; lauri.sydanheimo@tut.fi; leena.ukkonen@tut.fi).

M. M. Tentzeris is with the Georgia Institute of Technology, Atlanta, GA 30332-250 USA (e-mail: etentze@ece.gatech.edu).

Color versions of one or more of the figures in this letter are available online at http://ieeexplore.ieee.org.

Digital Object Identifier 10.1109/LAWP.2013.2270932

II. Design and Coding Technique

A. Design Details and Basic Principles

The proposed design has been optimized to be compatible with inkjet printing techniques. For proof of concept, we chose silver nanoparticle-based inks that feature the best realized conductivity values among most commonly used inkjet-printed inks. As shown in Fig. 1(a), to compensate conductivity losses, we used large strip widths of 4, 3, and 2.5 mm for the scatterers 1–3, respectively. The scatterer shape composing the tag in Fig. 1(a) relies on a dual-rhombic loop antenna. This structure has already been experimented in [5] to realize a sewn tag on fabric for different purposes. When an incident plane wave in vertical polarization impinges on a scatterer, it creates a wideband structural mode due to quasi-optical reflection of the incident wave and a resonant antenna mode due to induced currents. This last mode is involved in the generation of the ID. A first resonant mode (antenna mode) appears when the wavelength is equal to half of the total length of the loop. It is to be noted that, for this design, in horizontal polarization the electromagnetic response shows a wideband response that cannot be used for ID purpose.

The induced surface currents shown in Fig. 2(a) create a maximum reflection at the first resonant frequency. Fig. 2(c) shows the RCS 3-D pattern obtained for an incident plane wave normal to the tag surface. It can be observed that the main power is reflected toward and backward of the source of the plane wave. We can extract a half-power beamwidth (HPBW) of 84° and 70.7° at resonance frequency (3.45 GHz) in H-plane and E-plane, respectively. This means that the tag can be detected in reflection, either in monostatic configuration with a single antenna or in bistatic configuration with two separate antennas. However, a

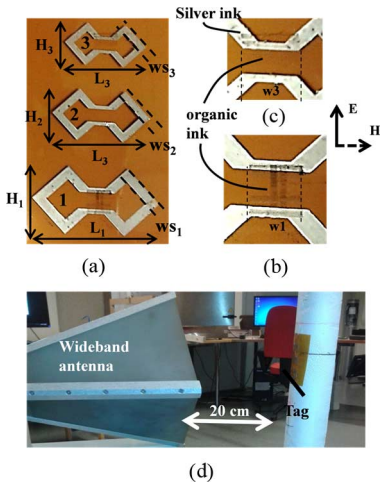

Fig. 1. (a) Photograph of the tag based on multiple dual-rhombic scatterers realized by inkjet printing. (b) Zoom on resistive strip of scatterer 1. (c) Zoom on resistive strip of scatterer 3. (d) View of the measurement setup. The dimensions of the scatterers are $L_1 = 41.5$ mm, $H_1 = 22.1$ mm, $L_2 = 32.4$ mm, $H_2 = 17.2$ mm, $L_3 = 27$ mm, $H_3 = 14.4$ mm, $ws_1 = 4$ mm, $ws_2 = 3$ mm, $ws_3 = 2.5$ mm.

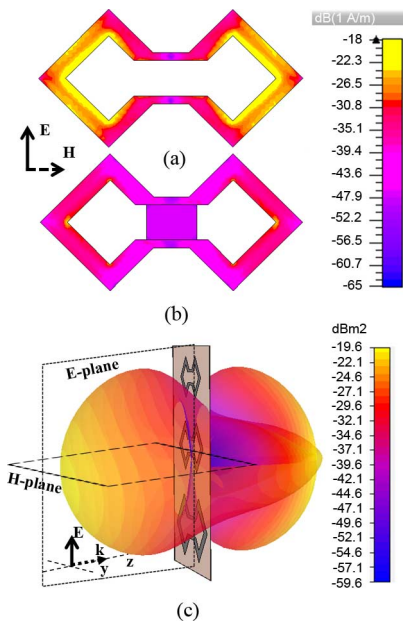

Fig. 2. Surface currents for the scatterer 1 at resonant frequency (3.45 GHz). (a) Without resistive strip. (b) With a resistive strip width of $w_1 = 8$ mm. The bridging resistance value is $1025\ \Omega$. (c) $|\mathrm{RCS}|$ 3-D pattern in vertical polarization obtained for an incident plane wave normal to the tag, at 3.45 GHz.

detection in transmission could be hardly implemented because the rear beam presents zeros for some angles.

The chipless tag of Fig. 1(a) is composed of three scatterers with various sizes to create three resonant peaks (for the "no resistive ink" case) as shown in Fig. 3(a). The overall size of the tag is 7×4 cm^2, which is still compatible with the credit card format of 8.5×5.4 cm^2. Using a higher number of scatterers is possible, at the expense of a larger design. The targeted resonant frequencies are 3.5, 4.4, and 5.3 GHz for scatterers 1–3, respectively. This gives an equal-frequency separation of 900 MHz that is a minimum for a good decoupling of the three resonant modes. This allows obtaining a significant

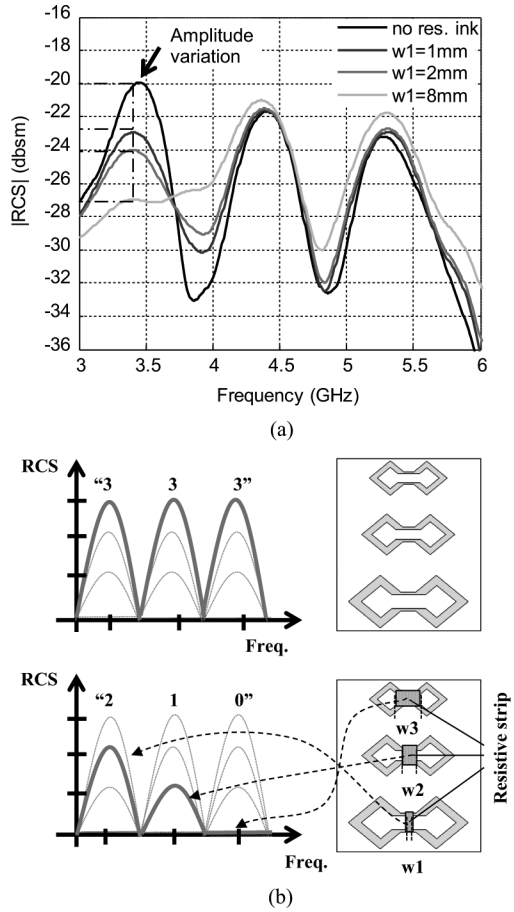

Fig. 3. (a) $|\mathrm{RCS}|$ simulation results of the tag for various resistive strips width w_1 deposited on the scatterer 1. These results have been obtained with the help of CST Microwave Studio. (b) Amplitude shift keying principle.

peak height of 10 dB, correlated with the bandwidth of each resonator, that is mandatory for an ASK coding technique. A separation of 8 mm between each scatterer allows for the decoupling of the three resonant peaks involved in the generation of the ID. The scatterers are stacked along the vertical axis that is beneficial to maximize the radar cross section (RCS) value because the structural mode of reflection is stronger when the largest dimension of the substrate is aligned with the polarization vector. First, the design of a single scatterer was optimized at 3.5 GHz. Then, a scaling factor in two dimensions (x-y) is applied for the two others scatterers in order to modify the resonant frequency while maintaining an almost constant quality factor equal to 10 due to their self-similar shapes. The RCS values at resonance are -20, -22, and -23 dBsm for the peaks 1–3, respectively. We noticed that the magnitude of the backscattered response depends on the incident angle of the interrogating wave in H-plane because the structural mode is strongly affected. However, the resonant peaks can still be clearly distinguished. This enables the detection of tags for various incident angles.

B. ASK Coding Technique Principle and Implementation

For the current work, to generate the ID, we experiment with a novel technique to enhance coding efficiency when the quality factors of resonant peaks are relatively low (e.g., when using high-loss substrates and conductive strips). It consists in varying

the amplitude of each resonant peak to increase the number of coding states for each scatterer. For this purpose, we noticed that when shorting the dual-rhombic loop scatterer in the middle, with a resistive strip [see Figs. 1(a) and 2(b)], one can obtain a peak magnitude correlated with the "bridging" resistance value. Fig. 3(a) shows the RCS as a function of frequency for several tag configurations for which only the first resonant peak is affected due to the width variation of the resistive deposit on top of scatterer 1. When the resistance becomes low, the resonant peak vanishes. Fig. 2(b) shows that surface currents are now homogenous in the middle and in the diamond loops. The intensity is lower, compared to the case with no resistive strip, so this explains the resonance cancellation. The coding principle based on amplitude shift keying for each resonant peak is described in Fig. 3(b) for a tag having $k = 3$ scatterers. For each peak, we define a number of states N, from the minimum value that is "no peak" to the maximum value when the resistance is infinite (no resistive strip printed). In this example, each peak magnitude can evolve between four values, so that two bits can be encoded. Equation (1) allows for the calculation of the coding capacity C in bits for k resonant peaks, as a function of the magnitude deviation ΔM between maximum and minimum values, and the magnitude resolution dM. According to (1), in Fig. 3(b) the resulting capacity is 6 bits

$$C = \log_2\left(\left(\frac{\Delta M}{dM} + 1\right)^k\right) \tag{1}$$

$$C = \log_2\left(\prod_{i=1}^{k}\left(\frac{\Delta M_i}{dM_i} + 1\right)\right) \tag{2}$$

$$C = \log_2\left(\left(\frac{\Delta M_1}{dM_1} + 1\right)\cdot\left(\frac{\Delta M_2}{dM_2} + 1\right)\cdot\left(\frac{\Delta M_3}{dM_3} + 1\right)\right). \tag{3}$$

For the current design, in Fig. 3(a), ΔM corresponds to 7 dB of maximum deviation between -20 and -27 dBsm. The magnitude resolution dM is chosen to be 1 dB as a tradeoff between detection reliability when subject to a noisy environment and coding density. This gives theoretically eight combinations for the first resonant peak. However, the amplitude variation of the first resonant peak affects a little the other resonant peaks. Indeed, when the first resonant peak is canceled, variations of 0.5 and 1 dB can be seen on the second and the third resonant peaks, respectively. This means that (1) has to be rewritten in (2) in the general case for which each peak of index i has different magnitude resolution and maximum deviation. For the present design having three resonant peaks of index $i = 1$ to 3, (3) can be derived from (2). The magnitude resolution of peaks 2 and 3 are chosen to 1.5 and 2 dB, respectively. The peak 2 can vary between -22 and -30 dBsm, and the peak 3 between -23 and -30 dBsm. Based on these values, from (3) we obtain a total number of combinations equal to $8 \times 5x3 = 120$—that is, 6.9 bits.

A good mean to create a resistive strip is to use an organic ink featuring a much lower conductivity compared to metallic nanoparticles-based ink. We created localized resistive shorts with the help of a commercial CNT-doped PEDOT-PSS organic ink from Poly-ink Company. We found experimentally that a sheet resistance of $1000\,\Omega/\text{sq}$ can be obtained with a 1-μm-thick single layer of ink. Once deposited, the ink is quasi-transparent as shown in Fig. 1(a)–(c), so that it is difficult to read the tag ID only with visual inspection. This interesting behavior can be beneficial for anti-counterfeiting applications. To practically implement this coding technique, we can vary the resistive strip width (as denoted w_1, w_2, and w_3 in Fig. 3(b)) deposited for each scatterer. As observed in Fig. 3(a), if the resistive ink fully covers the gap of scatterer 1 ($w_1 = 8$ mm), the resonant peak disappears. On the other hand, the peak magnitude is maximum if no "bridging" organic ink is present. This provides the two opposite states. If the width of the strip is $w_1 = 1$ mm, for the largest scatterer, we obtain a 2-dB attenuation loss. Finally, a strip width of $w_1 = 2$ mm provides an attenuation of 3 dB compared to the "no resistive bridging strip" case. Here, it is observed that we can gradually decrease the level of response for a given frequency peak, as a function of the width of the resistive strip.

III. Results and Discussions

We realized the tag shown in Fig. 1(a) with the help of an inkjet printer Dimatix DMP-2831. To create the conductive strip, we used Harima Nanopaste silver nanoparticle ink featuring a maximum conductivity of 6.3 and 5 MS/m at 3.5 and 5.3 GHz, respectively. Two layers of silver ink have been printed followed by a sintering at 150°C for 1 h. The thickness of the two-layer silver-ink deposition strip is roughly approximated to be close to 2 μm. The substrate used is polyimide ($\varepsilon_r = 3.5$, $\tan\delta = 0.0027$) 0.1 mm thick. Then, the deposit of the SWCNT/PEDOT-PSS-based organic ink has been done several times, to vary for each step the resistive strip width as shown in Fig. 1(b) and (c) for the scatterers 1 and 3, respectively. It is noteworthy that no sintering is required after printing. This makes the configuration of a "virgin" tag (having the initial code "0") quick and inexpensive.

To extract the electromagnetic response of a chipless tag as a function of frequency, we can either implement a frequency-modulated continuous wave (FMCW) radar technique [6] or a frequency-stepped continuous wave (FSCW) radar technique used in this letter. The radar sends a continuous wave toward the remote chipless tag and detects the backscattered power for several frequency points in the band of interest. We used the vector network analyzer (VNA) Agilent PNA E8358A connected to a wideband antenna ETS Lindgren 3164–04 having a gain between 9 and 12 dBi from 3 to 6 GHz, shown in Fig. 1(d). The port 1 of the VNA is connected to the vertical polarization input of the antenna, the tag being aligned with the vertical axis as in Fig. 1(d). The record of the parameter S_{11} provides indirectly the tag's response using a free-space calibration technique, explained in [4]. It relies upon the initial record of the clutter map of the background and of a known scatterer (metallic rectangular plate) to deembed the gain nonuniformity over the frequency range. The transmitting power delivered by the VNA is 0 dBm. The sensitivity of the receiver is limited by the noise floor level and was found at -80 dBm with an IF bandwidth of 1000 Hz. The chipless tag is placed on a polystyrene stand 20 cm away from the antenna aperture. With the aforementioned parameters, the minimum RCS detectable is close to -45 dBsm.

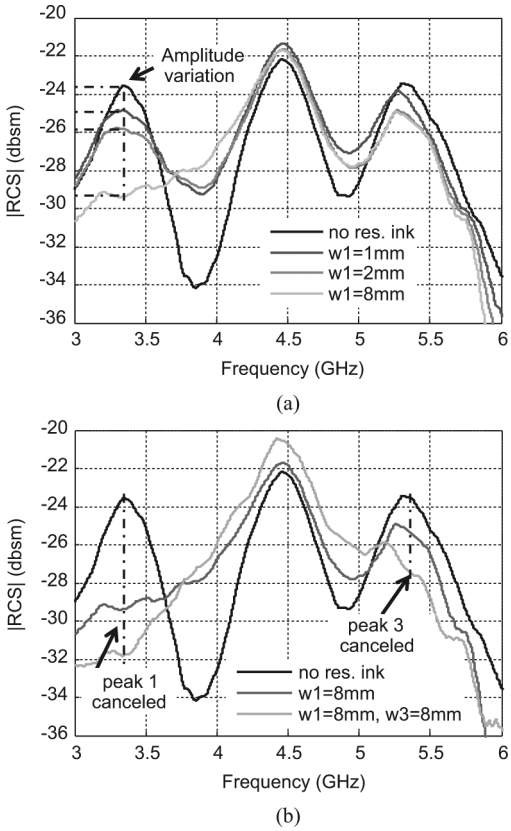

Fig. 4. $|\mathrm{RCS}|$ measurements results for various configurations. (a) Different amounts of CNT are deposited in several steps to create different levels of damping on the first resonant peak. (b) Large surface is deposited on some of the scatterers to make the resonant peak fully vanish.

Fig. 4(a) shows RCS measurement results, carried out in an indoor environment, for three configurations that clearly demonstrate the effect of the resistive strip width variation on top of scatterer 1. With no CNT deposit, the magnitude of the first resonant peak is close to -23 dBsm. The presence of the resistive strips of widths 1 and 2 mm decreases the RCS to -25 and -26 dBsm, respectively. On the other hand, when the resistive strip width is 8 mm, the peak is not visible anymore with a level close to -30 dBsm. Thus, the span is 6 dBsm between the maximum and the minimum value, and variations of 1 dB are clearly visible. This value is very close to those obtained in simulation [see Fig. 3(a)]. It is to be noted that 1 dB of resolution can be achieved in a practical environment using the free-space calibration aforementioned. The surrounding-clutter-related RCS fluctuation has to be kept lower than 0.5 dB. This is the case when the detection environment is static (objects not mobile). To allow for a reliable detection of the difference peak height in a more usual identification environment and avoid false detection, additional signal processing technique such as time gating can mitigate the RCS fluctuation. Moreover, the use of a high focusing beam antenna that limits the detection area around the tag may improve the background isolation.

It is noteworthy that the other resonant peaks do not show any significant magnitude variation, except for the peak at 5.3 GHz that loses 1 dB, when the first peak is removed. Fig. 4(b) shows measurements results to compare the "no strip" response to resistive strip configurations that fully cancel the resonant peaks. The contrast between minimum and maximum RCS values is well detectable. It confirms that if the middle gaps of both scatterers 1 and 3 are fully covered by resistive organic inks, only the resonant peak at 4.4 GHz can be detected. These measurements are in good agreement with simulations results. They confirm the possibility to implement an ASK coding technique with the help of resistive ink.

IV. Conclusion

This letter demonstrates that the combination of a conductive silver ink with a CNT-doped organic resistive ink could be an easy and inexpensive way to implement a novel coding technique for chipless RFIDs that is based on amplitude shift keying of independent resonant peaks. With three scatterers, more than 6 bits can be encoded. Furthermore, the use of organic ink makes the configuration of chipless tags flexible and easy to reconfigure as the organic ink can be added just as a second stage of inkjet printing, which does not require sintering. Finally, the organic ink is highly optically transparent, thus making the above configuration near-invisible, leading to completely different backscattering performances of chipless tags looking similar. Future works will aim to decrease the size of the tag as well as increase its coding capacity.

Acknowledgment

The authors thank the NSF and the NEDO Japan.

References

[1] K. Finkenzeller, *RFID Handbook: Fundamentals and Applications in Contactless Smart Cards, Radio Frequency Identification and Near-Field Communication*. Hoboken, NJ, USA: Wiley, 2010.

[2] A. Ramos, D. Girbau, A. Lazaro, and S. Rima, "IR-UWB radar system and tag design for time-coded chipless RFID," in *Proc. 6th Eur. Conf. Antennas Propag.*, Mar. 2012, pp. 2491–2494.

[3] I. Jalaly and D. Robertson, "RF barcodes using multiple frequency bands," in *IEEE Int. Microw. Symp. Dig.*, Long Beach, CA, USA, Jun. 2005, pp. 139–142.

[4] A. Vena, E. Perret, and S. Tedjini, "Chipless RFID tag using hybrid coding technique," *IEEE Trans. Microw. Theory Tech.*, vol. 59, no. 12, pp. 3356–3364, Dec. 2011.

[5] A. Vena, E. Moradi, K. Koski, A. A. Babar, L. Sydänheimo, L. Ukkonen, and M. M. Tentzeris, "Design and realization of stretchable sewn chipless RFID tags and sensors for wearable applications," in *Proc. IEEE Int. Conf. RFID*, Orlando, FL, USA, Apr. 2013, pp. 176–183.

[6] H. Aubert, F. Chebila, M. Jatlaoui, T. Thai, H. Hallil, A. Traille, S. Bouaziz, A. Rifai, P. Pons, P. Menini, and M. Tentzeris, "Wireless sensing and identification of passive electromagnetic sensors based on millimetre-wave FMCW RADAR," in *Proc. IEEE RFID-TA*, Nov. 5–7, 2012, pp. 398–403.